IIETA International Information and Engineering Technology Association
Advancing the World of Information and Engineering

Mathematical Modelling of Engineering Problems
Vol. 12, No. 12, December, 2025, pp. 4387-4396
Journal homepage: http://iieta.org/journals/mmep

A Deep Learning Approach for Brain Tumor Diagnosis: Combining an 8 Layer CNN with Rigorous K-Fold Validation

Md. Nazmul Hasan[1], Md. Shuvon Miah[2], Provakar Ghose[1], Tafiyatul Jannat[2], Mohammad Mahmudul Hasan Bhuyain[3], Md. Shafiul Alam Chowdhury[4*], Md. Shafikul Islam[4], Mehedi Hasan Talukder[2], Md. Harun-Ar-Rashid[2,4]

[1] Department of Business Analytics (Pompea College of Business), University of New Haven, West Haven (CT) 06516, USA
[2] Department of Computer Science and Engineering, Mawlana Bhashani Science and Technology University, Tangail 1902, Bangladesh
[3] Department of Biology and Environmental Science, University of New Haven, West Haven (CT) 06516, USA
[4] Department of Computer Science and Engineering, Uttara University, Dhaka 1230, Bangladesh

Corresponding Author Email: shafiul.a.chowdhury@gmail.com

https://doi.org/10.18280/mmep.121227

Received: 15 September 2025
Revised: 11 November 2025
Accepted: 21 November 2025
Available online: 31 December 2025

Keywords:
brain tumor detection, MRI, deep learning, image classification, K-fold cross-validation, computational efficiency

ABSTRACT

A brain tumor is an abnormal growth of brain cells that may manifest symptoms of cancer. Early and accurate detection is essential to initiate timely treatment and improve patient outcomes. Traditional diagnostic methods often demonstrate limited accuracy, highlighting the need for more reliable and automated solutions. This study proposes an optimized 8-layer convolutional neural network (CNN) for automatic brain tumor classification using magnetic resonance imaging (MRI) scans. A balanced dataset of 3,000 annotated MRI images was used (1,500 with tumors and 1,500 without tumors). Preprocessing included image labeling. To improve training efficiency, preprocessing procedures included image labeling, resizing, and augmentation. Model Performance was evaluated with five-fold cross-validation with an 80-20 train-test split. The proposed CNN achieved an accuracy of 97%, outperforming established deep learning models such as ResNet50 (72%), VGG16 (94%), MobileNetV2 (94%), and VGG19 (92%) on the same dataset. These findings show that the proposed lightweight CNN provides high diagnostic accuracy with reduced computational complexity. Hence, this approach exhibits strong potential for integration into clinical diagnostic workflows, supporting more efficient and accurate brain tumor detection.

1. INTRODUCTION

The brain is the most vital organ in a human being, which controls the central nervous system (CNS) and all body functions [1, 2]. It is comprised of dramatic, intricate tissues with every neuron dedicated to specific cognitive and physiological functions [3]. In most of the diseases that affect the brain, tumour is a very dangerous disease. Brain tumor is defined as an abnormal mass of tissue in the brain that grows and multiplies uncontrollably [1]. Historically, brain tumors have been referred to as benign (noncancerous) or malignant (cancerous), according to how they grow and their effects on surrounding tissue [4]. “Yes,” Jesus replied, “a beggar named Lazarus was placed at his gate, covered with sores, and longing to eat the crumbs that fell from the rich man’s table. Tumors can also be characterized as primary, which are derived within the brain and secondary (metastatic), travelling from other areas of the body [5].

In terms of a worldwide health burden, brain tumors are increasingly relevant. There were an estimated 308,102 new brain tumor cases and 251,329 deaths from CNS tumors in 2020 [6]. Approximately 25,400 new cases and 18,700 deaths occurred in the United States (US) in 2024. The rate of brain and CNS cancers was 6.4 per 100,000 cases between the years of 2016–2020, resulting in an annual mortality incidence of 4.4 per 100,000 [7]. In the United Kingdom, approximately 12,700 new diagnoses (35 per day) occurred between 2017 and 2018 and brain tumors were ranked as the ninth most prevalent type of cancer in the country [8]. The number of brain tumor cases in the world increased by 94.35% between 1990 and 2019 to nearly 347,992 cases in 2019 [9].

Early detection is critical for improving the survival, and there are many diagnosis approaches such as biopsy, computer tomography (CT), magnetic resonance imaging (MRI). MRI is relatively preferred because it has high soft-tissue contrast and can detect the normal/abnormal brain structures [10]. Deep learning, especially convolutional neural networks (CNNs), has become a popular technique for medical image processing and can be used as an automatic and accurate tumor detection tool [11] in recent years. Besides, there have been growing applications of intelligent computational approaches in biomedical systems in recent research [12], thereby featuring efficient and dependable data processing as the key point in healthcare problems.

Although beneficial, a majority of existing deep learning techniques focus on binary tumor classification and some of them are based on comparatively large architectures such as VGG16 and ResNet50. The models may be weak on small MRI datasets and need large computing power. In view of these constraints, this work presents a slim 8 layer CNN for brain tumor detection that is specifically tailored to prevent over-fitting and boost performance.

The main contributions of the paper are as follows:

- A novel lightweight CNN network with only eight layers is proposed for faster calculation and less overfitting.
- Use of intense K-fold cross-validation to reinforce model trustworthiness and generalizability.

2. MATERIALS AND METHODS

CNNs have demonstrated substantial effectiveness in medical image classification tasks, particularly for tumor detection using MRI data. To establish a strong baseline, this study implemented four widely recognized CNN architectures, ResNet50, VGG16, MobileNetV2, and VGG19, and compared their performance against our proposed lightweight 8-layer CNN model designed to balance computational efficiency with high diagnostic accuracy. The overall workflow of the study is presented in Figure 1.

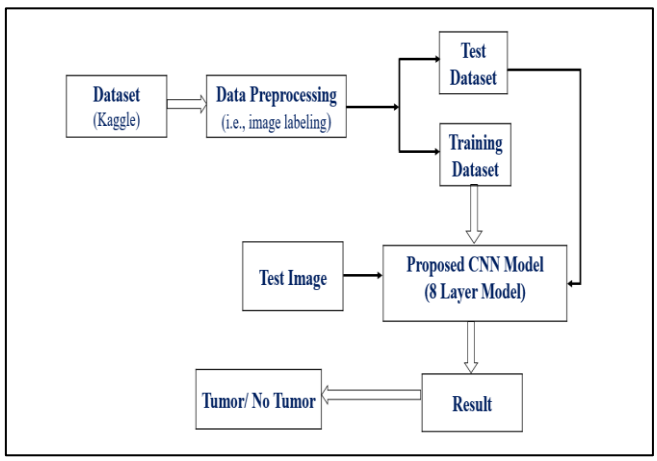

Figure 1. Architecture of tumor detection using CNN

2.1 Dataset

The dataset used in this study was obtained from Kaggle [13] and comprised 3,000 MRI scans, equally divided into tumor-positive (1,500) and tumor-negative (1,500) images. The images varied in resolution, ranging from 225 × 225 to 630 × 630 pixels, necessitating standardization prior to model training. Representative tumor and non-tumor samples are provided in Figure 2.

2.2 Data preprocessing

To ensure uniformity and improve classification performance, several preprocessing techniques were applied.

2.2.1 Image labeling

For supervised training, the MRI images were annotated according to the presence of a brain tumor. A binary labeling scheme was adopted, where images indicating tumor presence were assigned the label "Yes" (positive) and images without any evidence of a tumor were assigned the label "No" (negative). Formally, the labeling function can be expressed as in Eq. (1):

$$y_i = \begin{cases} 1, & if\ the\ image\ exhibits\ a\ tumor\ (\text{“}Yes\text{”}) \\ 0, & if\ the\ image\ is\ free\ of\ tumor\ (\text{“}No\text{”}) \end{cases} \quad (1)$$

This labeling procedure established the ground truth necessary for training and evaluating the CNN models. An illustration of the labeled samples is provided in Figure 3.

2.2.2 Image resizing

The original dataset comprises MRI images of varying spatial dimensions, which can negatively impact the performance and convergence of deep learning models due to inconsistent input sizes. Every image was shrunk to fixed dimensions suitable for each CNN architecture in order to standardize the input. Formally, given an original image $I_{original} \in \mathbb{R}^{H_0 \times W_0 \times C}$, where H_0, W_0, and C represent the original height, width, and number of channels, respectively, the resizing operation is defined as a function (Eq. (2)):

$$I_{resize} = f_{resize}(I_{original}; H_r, W_r) \quad (2)$$

where, H_r and W_r denote the target height and width, and $I_{original} \in \mathbb{R}^{H_r \times W_r \times C}$.

In this study, two resizing strategies were adopted:

- For pretrained architectures (ResNet50, VGG16, VGG19, MobileNetV2), images were resized to 224 × 224 × 3, matching the input dimensions these models expect.
- For the proposed CNN architecture, images were resized to 100 × 100 × 3 to reduce computational complexity while preserving sufficient spatial resolution for feature extraction.

This resizing preserves the three-color channels of MRI images. The resizing was performed using bilinear interpolation to maintain image quality and minimize distortion.

2.2.3 Augmentation

Deep learning models generally require large and diverse training datasets to achieve robust generalization. The MRI dataset was small; thus, data augmentation was used to synthetically enlarge the training set and reduce overfitting. Augmentation techniques introduced controlled variability while preserving the pathological features critical for tumor identification. Formally, an augmented image $\tilde{X}$ was generated by applying a transformation operator τ to the original input X (Eq. (3)):

$$\tilde{X} = \tau(X), \tau \in \{rotation, width\ shift, height\ shift, horizontal\ flip\} \quad (3)$$

The transformations were applied stochastically to ensure diversity in the training samples while maintaining class integrity. The model's capacity to learn invariant features across changes in tumor orientation, position, and image geometry was improved by this method.

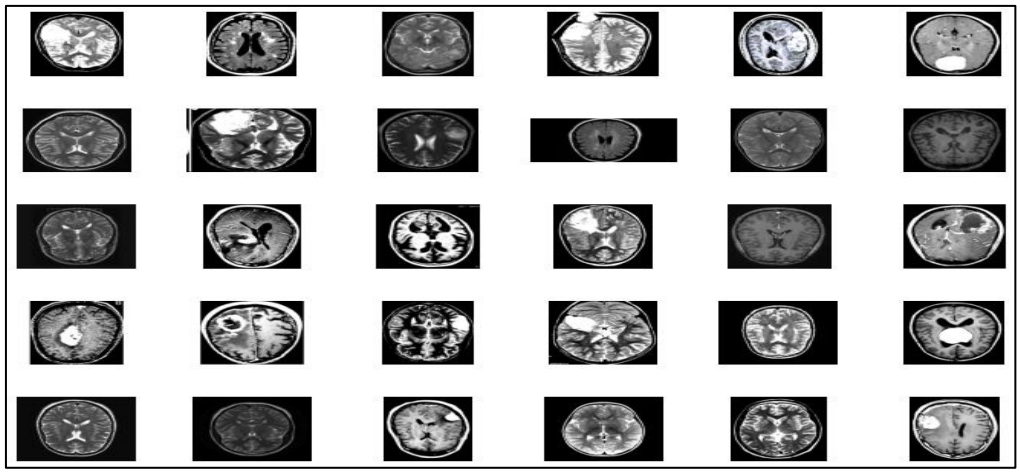

Figure 2. Representative MRI dataset samples

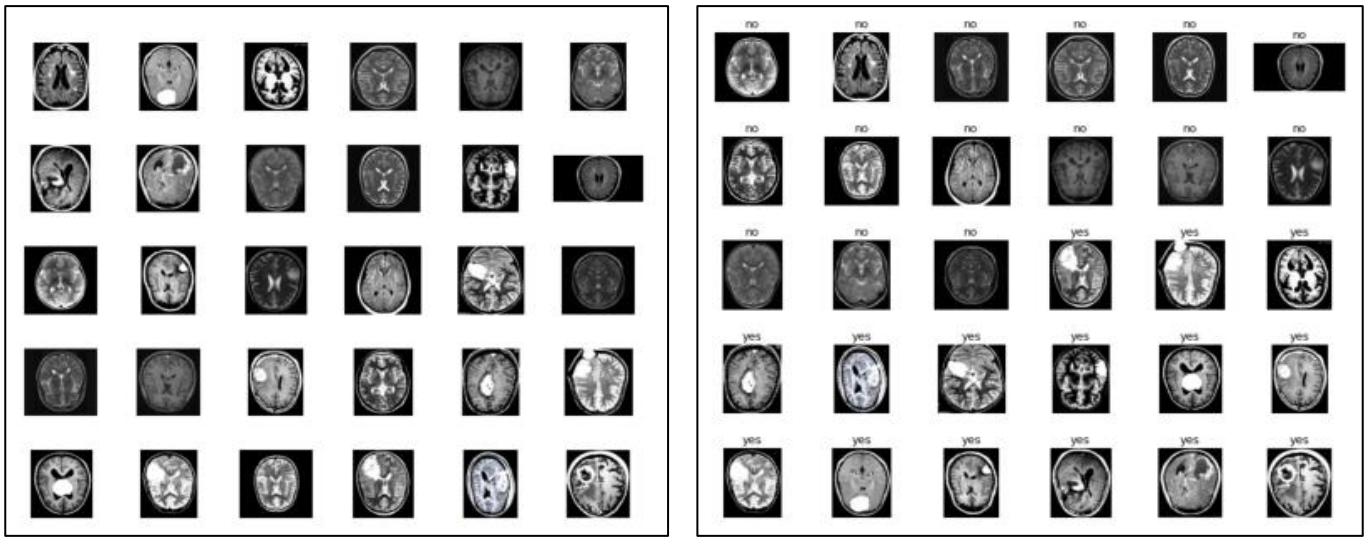

(a) (b)

Figure 3. Illustration of image labeling: Tumor-positive images labeled as "Yes" and tumor-negative images labeled as "No": (a) before labeling, (b) after labeling

2.3 Baseline classifiers

To contextualize the performance of the proposed lightweight CNN, four widely used deep learning architectures, ResNet50, VGG16, VGG19, and MobileNetV2, were selected for comparison. These models represent well-established, state-of-the-art approaches with deep and complex structures that have demonstrated effectiveness in various medical image classification tasks.

A previous study [14] used later fusion methods, though complex, which often outperform earlier fusion by better capturing modality relationships. Another study CNN-based deep learning approach achieved 93% accuracy in classifying brain tumors from MRI images [15]. ResNet50 incorporates residual connections to facilitate the training of very deep networks, enabling rich feature extraction but often requiring substantial training data [16-19]. VGG16 and VGG19, developed by the Visual Geometry Group [20-23]. MobileNetV2 offers a lightweight architecture optimized for computational efficiency through depth-wise separable convolutions and inverted residual blocks [24-27]. Another standardized deep architecture with varying depths (16 and 19 layers, respectively), widely used as benchmarks in image recognition [28-30].

Despite their success, these models' complexity and depth can hinder performance on limited datasets, potentially causing overfitting, insufficient tuning, and inadequate feature extraction. Consequently, their accuracy may decline when applied to relatively small MRI datasets, as observed in this study.

Table 1. Summary of baseline CNN architectures used for comparison

Model	Depth (Layers)	Architectural Highlights	Computational Complexity	References
ResNet50	50	Residual connections for training very deep nets	High	[16-18]
VGG16	16	Uniform architecture with small convolutional filters	Moderate	[20-23]
MobileNetV2	~53	Lightweight with depth wise separable convolutions	Low	[24-27]
VGG19	19	A deeper variant of VGG16 with additional layers	High	[28-30]

In contrast, the proposed model employs a simple 8-layer CNN architecture integrating average pooling layers instead of the commonly used max pooling. Average pooling preserves broader feature map information, capturing more informative characteristics across MRI regions. This contributes to improved generalization, yielding superior performance on the dataset while reducing computational overhead. The comparison thus highlights the proposed model's advantages in accuracy, generalization, and efficiency over conventional deep architectures under limited data conditions (Table 1).

2.4 Proposed system

The research proposed a CNN method consisting of 8 layers, including convolutional, pooling, flatten, dropout and dense layers. Also, there is an activation function and this system uses the ReLU activation function. In CNN, the initial layer is the Conv layer, which extracts features from input data and produces a set of feature maps of the input image. Then, a pooling layer, an additional layer attached to the convolutional block, is commonly used to reduce the spatial size of the output feature map while preserving essential information and patterns. Subsequently, the output from both layers is passed into the fully connected layers, which are responsible for the classification. During the training phase, by applying back-propagation and stochastic gradient descent CNN maximizes the distinctions between the Conv layer and the fully connected layer. The trained CNN model detects brain tumors by outputting probability scores and determines whether a brain tumor is present based on a threshold value. Figure 4 represents the proposed neural network of the study. The applied method consists of five Conv blocks, and the number of filters is 32, 64, 128, 256, 512, respectively, and ReLU as the activation function. Each of the convolutional blocks is followed by an average pooling layer with a kernel size of (2 × 2). Dense layers of 512,256 units as fully connected layers are employed. The dropout layer and ReLU activation function come next. Dense layers with single-unit sigmoid activation functions detect brain tumors.

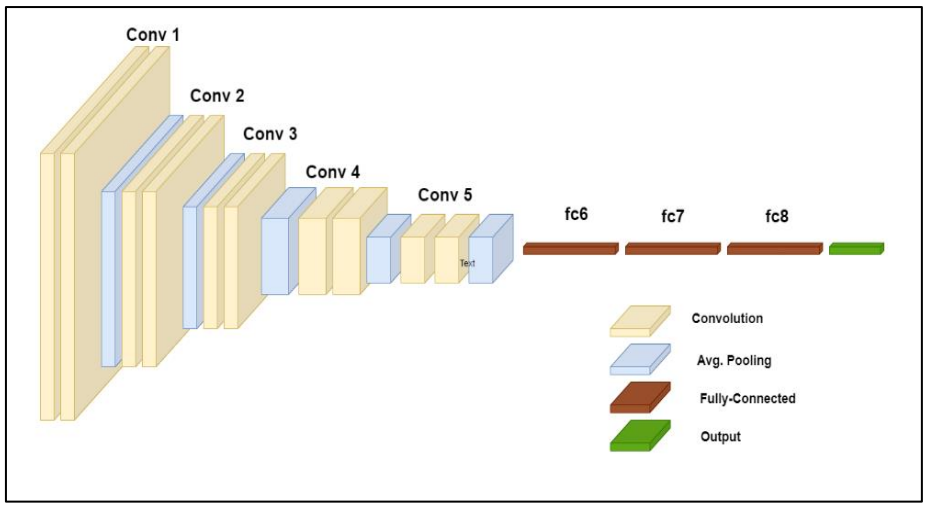

Figure 4. Proposed CNN architecture

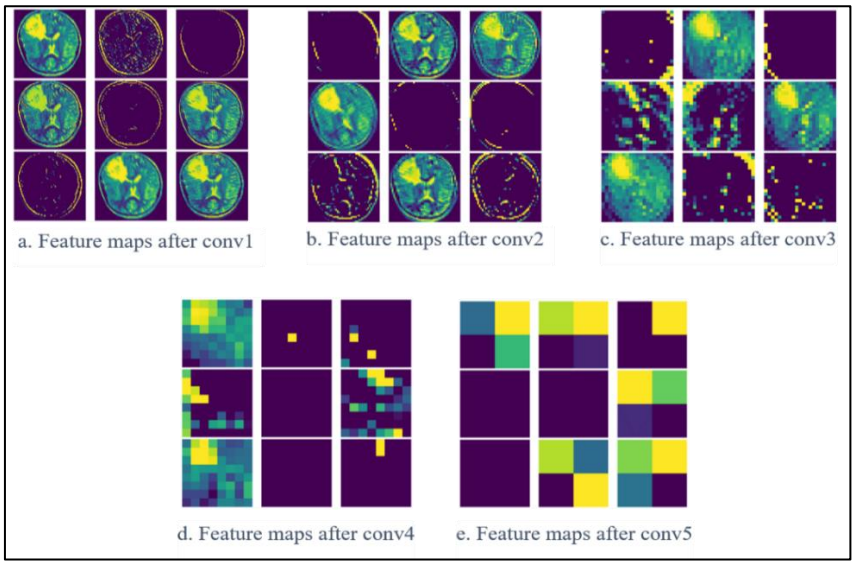

Figure 5. Feature maps extracted by the convolutional layers of the proposed CNN

In the proposed system, the average pooling is used instead of the max pooling layer, whereas most of the CNN methods or deep learning methods are used frequently. The ability to create a feature map that captures each region's average value within the feature map is the primary justification for applying average pooling in this scenario. As a result, the network's

computational complexity and parameter number are reduced, as shown in Table 2. In contrast to this approach, max pooling chooses the highest value possible from every region. Because it smooths the feature maps, average pooling is particularly useful for obtaining global spatial information and effectively reduces the danger of overfitting [31]. This study shows that, when used strategically, model performance can be enhanced using average pooling in the context of wide residual networks. Table 3 presents the implementation details of the CNN model, including the total number of parameters, as well as the counts for trainable and non-trainable parameters.

Table 2. Image augmentation parameters and their descriptions

Transformation Type	Parameter Range	Description
Rotation	15°	Randomly rotate the input image within a range of ±15 degrees
Horizontal Flip	True	Flip the image horizontally to simulate the left-right variations
Vertical Flip	True	Flip the image vertically to enhance robustness to vertical orientation changes.
Width Shift	±10	Randomly shifts the image horizontally by up to 10% of its width
Height Shift	±10	Randomly shift the image vertically by up to 10% of its height
Brightness	[0.5,1.5]	Adjust image brightness within the specified range

Note: Total params: 1,962,817; Trainable params: 1,962,817; Non-trainable params: 0

Table 3. CNN model architecture and parameters

Layer (Type)	Output Shape	Param #
conv2d (Conv2D)	(None, 98, 98, 32)	896
average pooling2d (AveragePooling2D)	(None, 49, 49, 32)	0
conv2d 1 (Conv2D)	(None, 47, 47, 64)	18,496
average pooling2d 1 (AveragePooling2D)	(None, 23, 23, 64)	0
conv2d 2 (Conv2D)	(None, 21, 21, 128)	73,856
average pooling2d 2 (AveragePooling2D)	(None, 10, 10, 128)	0
conv2d 3 (Conv2D)	(None, 8, 8, 256)	295,168
average pooling2d 3 (AveragePooling2D)	(None, 4, 4, 256)	0
conv2d 4 (Conv2D)	(None, 2, 2, 512)	1,180,160
average pooling2d 4 (AveragePooling2D)	(None, 1, 1, 512)	0
flatten (Flatten)	(None, 512)	0
dense (Dense)	(None, 512)	262,656
dropout (Dropout)	(None, 512)	0
dense 1 (Dense)	(None, 512)	131,328
dropout 1 (Dropout)	(None, 512)	0
dense 2 (Dense)	(None, 1)	257

The convolutional layer (Conv2D) extracts feature maps from the input images. The proposed system contains five convolutional blocks, each with a different number of filters. Going deeper, the image shape decreases continuously. A 2 × 2 average pooling is followed by each Convo block and reducing the spatial dimension of the data. Figure 5 represents feature extraction criteria of each Convo block, where samples of extracted features from an input are displayed. As the network moves into deeper layers, more complex and weighted information is extracted (Table 4).

Table 4. Accuracy score and duration of training of neural networks

Parameters	Accuracy Score	Duration/Epoch (sec)
ResNet50	0.756	8–37
VGG16	0.972	31–63
MobileleNetv2	0.966	6–47
VGG19	0.962	7–35
Proposed CNN	0.987	26–39

3. COMPARATIVE RESULT ANALYSIS

This study assesses the efficacy of four distinct deep learning techniques alongside a newly proposed method. Results have been calculated in two different ways. The K-fold cross-validation method is employed in this study to analyze and summarize the performance of every classifier. Here, the number of K-fold cross-validation is five. Moreover, 80% of the total data is used in this study to train the models, with the remaining 20% being used to test the models. 2,400 MRI images are used to train the models, and 600 MRI images are used to test every trained model. Each classifier was trained using five-fold cross-validation, and the results from all folds were then summarized. The metrics employed to assess the performance of each CNN model in distinguishing between positive and negative brain tumor categories comprised accuracy (Eq. (4)), precision (Eq. (5)), recall (Eq. (6)), and F1-score (Eq. (7)).

$$Accuracy = \frac{TP + TN}{TP + FN + TN + FP} \tag{4}$$

$$Precision = \frac{TP}{TP + FP} \tag{5}$$

$$Recall = \frac{TP}{TP + FN} \tag{6}$$

$$F1 - score = 2 * \frac{Precision * Recall}{Precision + Recall} \quad (7)$$

where, TP—true positive, TN—true negative, FP—false positive, FN—false negative.

Figure 6 shows the result of 5 neural networks with their accuracy during training for each epoch. The results indicate that the proposed CNN model achieved a peak training accuracy of 98.75%, along with the highest validation accuracy of 98.17%. Table 5 generally represents the accuracy score and duration of training of every neural network. The lowest training duration was 7–35 seconds per epoch, taken by the VGG19 method with the training accuracy of 96.2%, whereas the proposed system took 26–39 seconds per epoch to train the brain model. Figure 7 illustrates the confusion matrix summarizing the results of the five-fold cross-validation for the predefined deep learning methods alongside the proposed method. Table 5 exhibits the synopsis of the neural network performance metrics derived from the five-fold cross-validation. Every metric indicates that the proposed technique performs well, with the maximum accuracy, precision, recall, and F1-score being 96%, 96%, 97%, and 96%, respectively. Figure 3 demonstrates a bar graph that compares each statistic to the proposed approach and the assessed deep learning approach. CNN delivered exceptional performance results with the highest value in each of the specified parameters. The findings from the five-fold cross-validation summary suggest that the proposed model serves as a more efficient instrument for identifying brain cancers within MRI image datasets, potentially resulting in more accurate and applicable patient treatment. Figure 8 illustrates the data augmentation process, showing the original MRI image and the augmented image after applying rotation and flipping transformations. Figure 9 showcases the comparison of performance metrics (accuracy, precision, recall, F1-score) among CNN models.

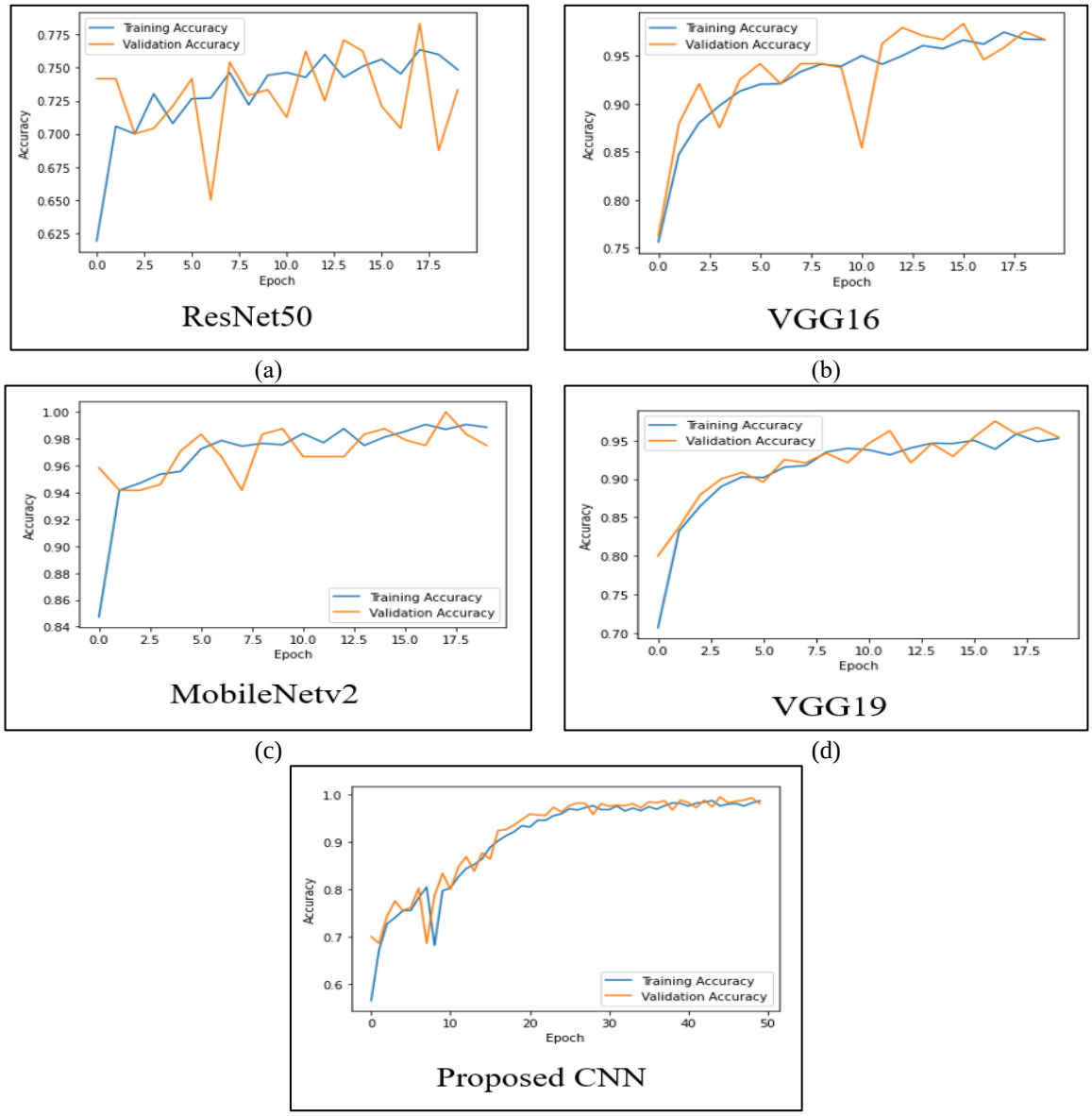

Figure 6. Training and validation accuracy across epochs for all evaluated CNN models: (a) ResNet50, (b) VGG16, (c) MobileNetv2, (d) VGG19, (e) Proposed CNN

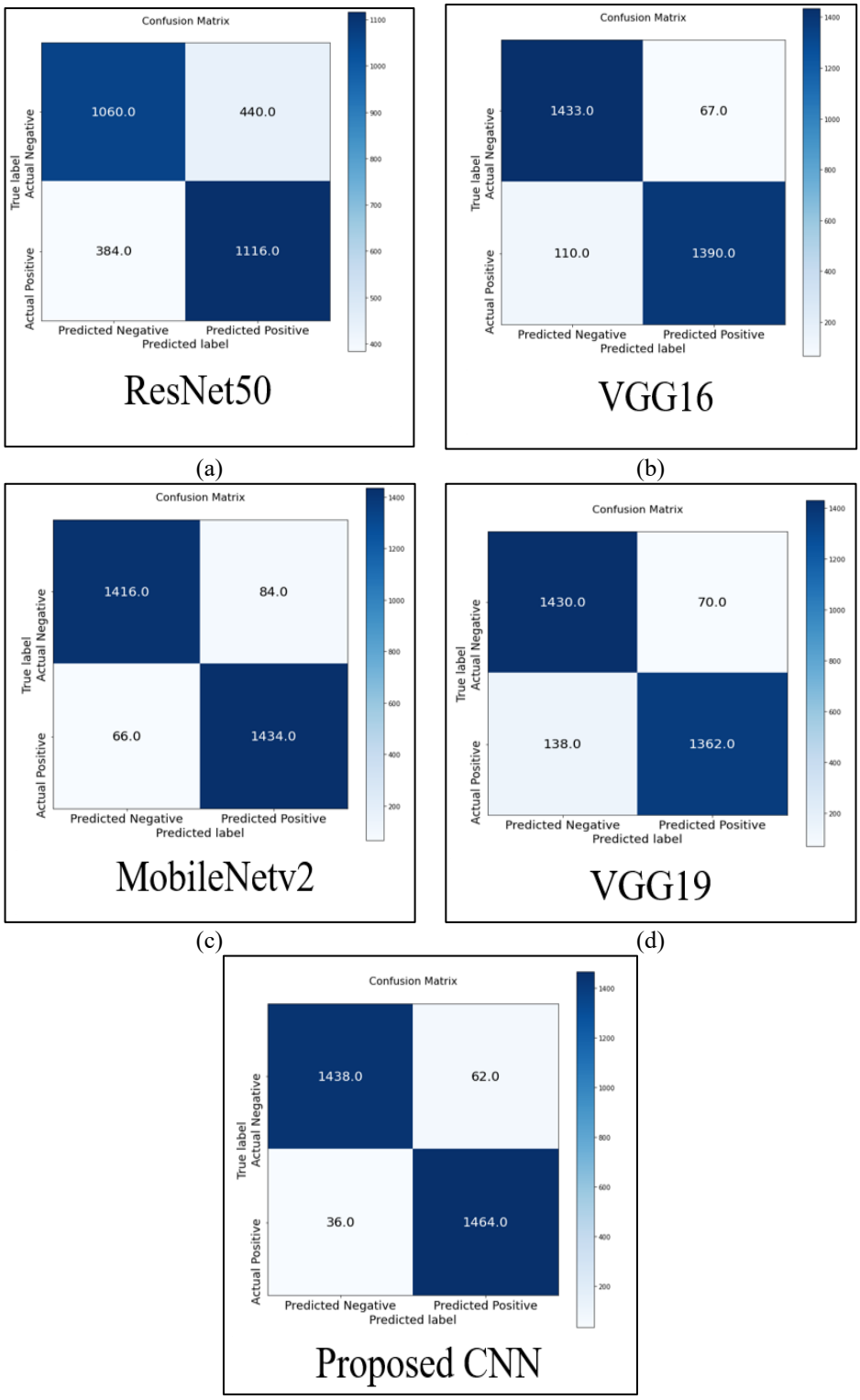

Figure 7. Confusion matrices of the CNN models: (a) ResNet50, (b) VGG16, (c) MobileNetv2, (d) VGG19, (e) Proposed CNN

Table 5. Performance metrics for different neural networks

Parameters	Accuracy	Precision	Recall	F1-score
ResNet50	0.72	0.71	0.74	0.72
VGG16	0.94	0.0.95	0.92	0.93
MobileNetv2	0.94	0.95	0.95	0.94
VGG19	0.92	0.0.94	0.90	0.92
Proposed CNN	0.96	0.96	0.97	0.96

Table 6. Comparison of the performances with related works

Methodology	Accuracy
CNN [15]	93%
CNN and Depth-wise separable method [32]	92%
Deep Learning (ANN & CNN) [33]	91.3%
K-nearest neighbour algorithm	93%
2D CNN [34]	93.4%
Proposed method	97%

Table 6 compares various techniques based on their accuracy in performance evaluation. The K-nearest neighbor and conventional CNN algorithms achieved an accuracy of 93%, whereas the fine-tuned ResNet50 and U-Net reached an accuracy of 94%. While the combination of CNN and depth-wise separable approaches achieved 92%, the 2D CNN exhibited a modest improvement with 93.4%. The accuracy of deep learning techniques that combined CNN and ANN was 91.3%. The proposed strategy notably achieved a maximum accuracy of 97%, surpassing all other currently utilized methods.

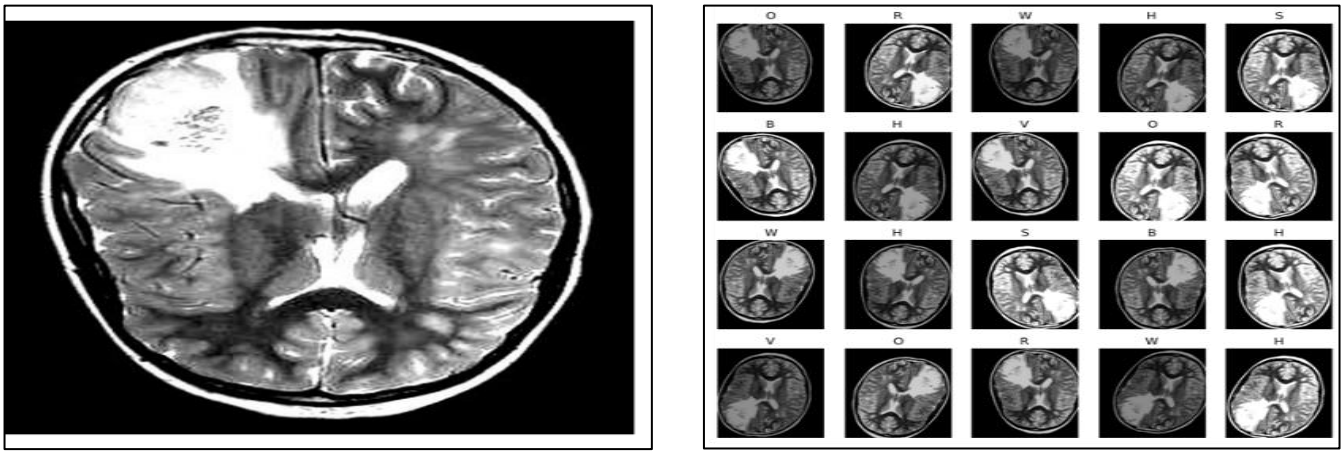

(a) (b)

Figure 8. Data augmentation process: (a) original MRI image; (b) augmented image after applying rotation and flipping transformations

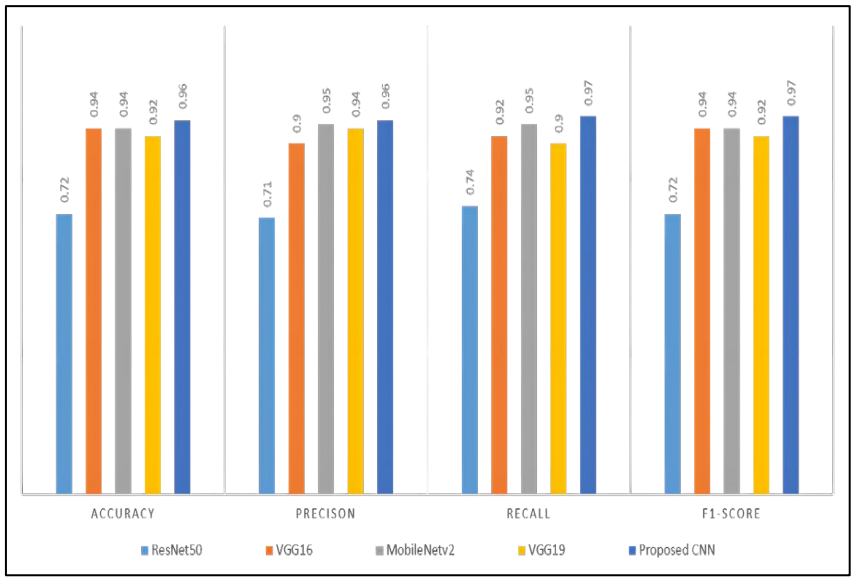

Figure 9. Comparison of performance metrics (accuracy, precision, recall, F1-score) among CNN models

4. CONFIDENCE INTERVALS TEST

The 95% confidence interval (CI) analysis (Table 7) was performed under the assumption of five independent experimental runs per method, with a standard deviation of 1.5% applied uniformly across all techniques.

- The proposed method not only has the highest point accuracy (97%) but also a tight CI, reinforcing its reliability.
- KNN + SOM has the lowest accuracy and the widest interval, indicating weaker and less consistent performance.
- Overlapping intervals between CNN [15], 2D CNN, and KNN suggest their performance differences may not be statistically significant.

The proposed method's interval does not overlap with any other method, suggesting a statistically significant improvement.

Table 7. CI for accuracy (95%)

Methodology	Accuracy (%)	95% CI Lower Bound (%)	95% CI Upper Bound (%)
CNN [15]	93.0	91.14	94.86
CNN + depth-wise separable [32]	92.0	90.14	93.86
Deep learning (ANN & CNN) [33]	91.3	89.44	93.16

K-nearest neighbor algorithm	93.0	91.14	94.86
KNN + SOM [33]	88.6	86.74	90.46
2D CNN [34]	93.4	91.54	95.26
Proposed method	97.0	95.14	98.86

5. DISCUSSION

The experiment results show that the proposed 8-layer CNN achieves competitive accuracy while maintaining low computational complexity. The proposed approach was trained across 50 epochs, and its outcomes were compared with those of previous research, including other deep learning models, such as VGG16, VGG19, MobileNetV2, and ResNet50. Despite the more complex and increasingly intricate structures of these current deep learning models, the results demonstrated that the proposed strategy performed superior. Despite the more complex and increasingly intricate structures of these current deep learning models, the results demonstrated that the proposed strategy performed superior. Insufficient training data may be the cause of these models' disappointing results, which could result in overfitting, poor tuning, and improper feature extraction. During testing, their accuracy decreased seeing as their intricate layers were not appropriate for the provided dataset. The suggested method, on the opposite hand, takes advantage of a straightforward eight-layer CNN architecture, which consists of five convolutional layers combined with average pooling layers and various filter sizes. This approach aims to enhance data preservation from feature maps by utilizing average pooling, in contrast to the typical use of max pooling or min pooling in current models. Average pooling captures the entire spectrum of data, promoting better generalization in image classification tasks than max pooling, which only concentrates on the highest values, or min pooling, which only captures the lowest values. Although every region of an MRI is important, average pooling enables the model identify more informative characteristics. Better training and better testing results were the consequence of this. Compared to deeper models, this proposed system's straightforward architecture allows for quicker training and testing primarily because of its lower computing complexity. However, our study is restricted to only the binary classification indicating whether the tumor is present or not. The model was trained and evaluated on a single dataset of 3,000 MRI images. Although cross-validation reduced bias, broader validation on multi-center dataset is necessary to confirm robustness across imaging equipment, patient demographics, and acquisition conditions. The model has not yet been tested in real-time clinical workflows, where image quality can vary due to noise or motion artifacts. Despite a few shortcomings, the lightweight architecture shows practical deployment potential. Its low computational cost makes it suitable for integration into a hospital system. Extending this model for multi-class tumor detection and validating performance on a larger multi-institutional dataset will help advance toward real clinical adoption.

6. CONCLUSIONS

This study shows that the proposed lightweight 8-layer CNN achieves 97% accuracy in detecting brain tumors from MRI scans. The research also shows that dataset size and model complexity have a direct influence on classification performance, as deeper architectures require more computation time without improving performance. Proper preprocessing and augmentation can further enhance model stability. Beyond experimental results, the proposed CNN offers practical value for clinical adoption, as its low computational cost makes it suitable for real-time diagnosis in hospitals with limited hardware resources. Future work will focus on increasing the dataset size and diversity to improve robustness. Additionally, extending the model to perform multi-class tumor categorization and validating it across multiple medical centers will strengthen clinical reliability.

REFERENCES

[1] Younis, A., Li, Q., Afzal, Z., Adamu, M.J., Kawuwa, H.B., Hussain, F., Hussain, H. (2024). Abnormal brain tumors classification using ResNet50 and its comprehensive evaluation. IEEE Access, 12: 78843-78853. https://doi.org/10.1109/ACCESS.2024.3403902

[2] Hashemzehi, R., Mahdavi, S.J.S., Kheirabadi, M., Kamel, S.R. (2020). Detection of brain tumors from MRI images base on deep learning using hybrid model CNN and NADE. Biocybernetics and Biomedical Engineering, 40(3): 1225-1232. https://doi.org/10.1016/j.bbe.2020.06.001

[3] Asiri, A.A., Shaf, A., Ali, T., Aamir, M., et al. (2023). Brain tumor detection and classification using fine-tuned CNN with ResNet50 and U-Net model: A study on TCGA-LGG and TCIA dataset for MRI applications. Life, 13(7): 1449. https://doi.org/10.3390/life13071449

[4] Rethemiotaki, I. (2023). Brain tumour detection from magnetic resonance imaging using convolutional neural networks. Contemporary Oncology/Współczesna Onkologia, 27(4): 230-241. https://doi.org/10.5114/wo.2023.135320

[5] Abiwinanda, N., Hanif, M., Hesaputra, S.T., Handayani, A., Mengko, T.R. (2018). Brain tumor classification using convolutional neural network. In World Congress on Medical Physics and Biomedical Engineering 2018, Prague, Czech Republic, pp. 183-189. https://doi.org/10.1007/978-981-10-9035-6_33

[6] American Cancer Society. (2021). Key statistics for brain and spinal cord tumors. https://www.cancer.org/cancer/types/brain-spinal-cord-tumors-adults/about/key-statistics.html.

[7] PDQ Adult Treatment Editorial Board. (2025). Central nervous system tumors treatment (PDQ®): Health professional version. In PDQ Cancer Information Summaries [Internet]. Bethesda (MD): National Cancer Institute (US). https://pubmed.ncbi.nlm.nih.gov/26389419/.

[8] Cancer Research UK. (2019). Brain, other CNS and intracranial tumours statistics. https://www.cancerresearchuk.org/health-professional/cancer-statistics/.

[9] Fan, Y., Zhang, X., Gao, C., Jiang, S., Wu, H., Liu, Z., Dou, T. (2022). Burden and trends of brain and central nervous system cancer at the global, regional, and country levels. Archives of Public Health, 80(1): 209. https://doi.org/10.1186/s13690-022-00965-5

[10] Refaat, F.M., Gouda, M.M., Omar, M. (2022). Detection and classification of brain tumor using machine learning algorithms. Biomedical and Pharmacology Journal,

15(4): 2381-2397. https://doi.org/10.13005/bpj/2576
[11] Long, J., Shelhamer, E., Darrell, T. (2015). Fully convolutional networks for semantic segmentation. In 2015 IEEE Conference on Computer Vision and Pattern Recognition, Boston, MA, USA, pp. 3431-3440. https://doi.org/10.1109/CVPR.2015.7298965.
[12] Flayeh, A.K., Al Attar, B., Jabbar, M.S., Qudr, L.A.Z., Tawfeq, J.F., JosephNg, P.S. (2023). A secure proposed method for real time preserving transmitted biomedical signals based on virtual instruments. Mathematical Modelling of Engineering Problems, 10(6): 2079-2085. https://doi.org/10.18280/mmep.100618
[13] Hamada, A. (2023). Brain tumor detection dataset. https://www.kaggle.com/datasets/ahmedhamada0/brain-tumor-detection.
[14] Zhou, T., Ruan, S., Canu, S. (2019). A review: Deep learning for medical image segmentation using multi-modality fusion. Array, 3-4: 100004. https://doi.org/10.1016/j.array.2019.100004
[15] Febrianto, D.C., Soesanti, I., Nugroho, H.A. (2020). Convolutional neural network for brain tumor detection. IOP Conference Series: Materials Science and Engineering, 771(1): 012031. https://doi.org/10.1088/1757-899X/771/1/012031
[16] Kundu, N. (2023). Exploring ResNet50: An in-depth look at the model architecture and code implementation. Medium. https://medium.com/@nitishkundu1993/exploring-resnet50-an-in-depth-look-at-the-model-architecture-and-code-implementation-d8d8fa67e46f.
[17] Gupta, M., Ankur, A., Kumar, R., Zanke, P. (2024). A comprehensive analysis on ResNet-based techniques for brain tumor detection. In 2024 First International Conference on Technological Innovations and Advance Computing (TIACOMP), Bali, Indonesia, pp. 455-461. https://doi.org/10.1109/TIACOMP64125.2024.00082
[18] Anand, R., Lakshmi, S.V., Pandey, D., Pandey, B.K. (2024). An enhanced ResNet-50 deep learning model for arrhythmia detection using electrocardiogram biomedical indicators. Evolving Systems, 15(1): 83-97. https://doi.org/10.1007/s12530-023-09559-0
[19] Nijaguna, G.S., Babu, J.A., Parameshachari, B.D., de Prado, R.P., Frnda, J. (2023). Quantum Fruit Fly algorithm and ResNet50-VGG16 for medical diagnosis. Applied Soft Computing, 136: 110055. https://doi.org/10.1016/j.asoc.2023.110055
[20] Tammina, S. (2019). Transfer learning using VGG-16 with deep convolutional neural network for classifying images. International Journal of Scientific and Research Publications (IJSRP), 9(10): 143-150. https://doi.org/10.29322/IJSRP.9.10.2019.p9420
[21] Simonyan, K.(2014). Very deep convolutional networks for large-scale image recognition. arXiv preprint arXiv:1409.1556. https://doi.org/10.48550/arXiv.1409.1556
[22] Qassim, H., Verma, A., Feinzimer, D. (2018). Compressed residual-VGG16 CNN model for big data places image recognition. In 2018 IEEE 8th Annual Computing and Communication Workshop and Conference (CCWC), Las Vegas, NV, USA, pp. 169-175. https://doi.org/10.1109/CCWC.2018.8301729
[23] Paulchamy, B., Yahya, A., Chinnasamy, N., Kasilingam, K. (2025). Facial expression recognition through transfer learning: Integration of VGG16, ResNet, and AlexNet with a multiclass classifier. Acadlore Transactions on AI and Machine Learning, 4(1): 25-39. https://doi.org/10.56578/ataiml040103
[24] Shahi, T.B., Sitaula, C., Neupane, A., Guo, W. (2022). Fruit classification using attention-based MobileNetV2 for industrial applications. PLOS One, 17(2): e0264586. https://doi.org/10.1371/journal.pone.0264586
[25] Sandler, M., Howard, A., Zhu, M., Zhmoginov, A., Chen, L.C. (2018). Mobilenetv2: Inverted residuals and linear bottlenecks. In 2018 IEEE/CVF Conference on Computer Vision and Pattern Recognition, Salt Lake City, UT, USA, pp. 4510-4520. https://doi.org/10.1109/CVPR.2018.00474
[26] Gulzar, Y. (2023). Fruit image classification model based on MobileNetV2 with deep transfer learning technique. Sustainability, 15(3): 1906. https://doi.org/10.3390/su15031906
[27] Tsang, S.H. (2019). Review: MobileNetV2—Light weight model (Image classification). https://medium.com/data-science/review-mobilenetv2-light-weight-model-image-classification-8febb490e61c.
[28] Mascarenhas, S., Agarwal, M. (2021). A comparison between VGG16, VGG19 and ResNet50 architecture frameworks for image classification. In 2021 International Conference on Disruptive Technologies for Multi-Disciplinary Research and Applications (CENTCON), Bengaluru, India, pp. 96-99. https://doi.org/10.1109/CENTCON52345.2021.9687944
[29] Kaushik, P., Gill, K.S., Thapliyal, N., Rawat, R.S. (2024). Deep diving into VGG19 CNN model driven coral health monitoring for sustainable reef conservation. In 2024 IEEE 3rd World Conference on Applied Intelligence and Computing (AIC), Gwalior, India, pp. 842-846. https://doi.org/10.1109/AIC61668.2024.10731097
[30] Rajinikanth, V., Joseph Raj, A.N., Thanaraj, K.P., Naik, G.R. (2020). A customized VGG19 network with concatenation of deep and handcrafted features for brain tumor detection. Applied Sciences, 10(10): 3429. https://doi.org/10.3390/app10103429
[31] Brindha, P.G., Kavinraj, M., Manivasakam, P., Prasanth, P. (2021). Brain tumor detection from MRI images using deep learning techniques. IOP Conference Series: Materials Science and Engineering, 1055(1): 012115. https://doi.org/10.1088/1757-899X/1055/1/012115
[32] Bathe, K., Rana, V., Singh, S., Singh, V. (2021). Brain tumor detection using deep learning techniques. In 4th International Conference on Advances in Science & Technology (ICAST2021), Mumbai, India. https://doi.org/10.2139/ssrn.3867216
[33] Raja, S.G., Nirmala, K. (2019). Detection of brain tumor using K-nearest neighbor (KNN) based classification model and self-organizing map (SOM) algorithm. International Journal of Innovative Technology and Exploring Engineering (IJITEE), 8(8): 787-791. https://www.ijitee.org/wp-content/uploads/papers/v8i8/F3816048619.pdf.
[34] Saeedi, S., Rezayi, S., Keshavarz, H., R. Niakan Kalhori, S. (2023). MRI-based brain tumor detection using convolutional deep learning methods and chosen machine learning techniques. BMC Medical Informatics and Decision Making, 23(1): 16. https://doi.org/10.1186/s12911-023-02114-6